Optimal Parameter Estimation in Heterogeneous Clutter for High-Resolution Polarimetric SAR Data

Gabriel Vasile, *Member, IEEE*, Frédéric Pascal, *Member, IEEE*, Jean-Philippe Ovarlez, *Member, IEEE*, Pierre Formont, *Student Member, IEEE*, and Michel Gay, *Member, IEEE*

***Abstract*—This letter presents a new estimation scheme for optimally deriving clutter parameters with high-resolution polarimetric synthetic aperture radar (POLSAR) data. The heterogeneous clutter in POLSAR data is described by the spherically invariant random vector model. Three parameters are introduced for the high-resolution POLSAR data clutter: the span, the normalized texture, and the speckle normalized covariance matrix. The asymptotic distribution of the novel span estimator is investigated. A novel heterogeneity test for the POLSAR clutter is also discussed. The proposed method is tested with airborne POLSAR images provided by the Office National d'Études et de Recherches Aerospatiales Radar Aéroporté Multi-spectral d'Etude des Signatures system.**

***Index Terms*—Detection, estimation, polarimetry, synthetic aperture radar (SAR).**

I. Introduction

THE RECENTLY launched polarimetric synthetic aperture radar (SAR) (POLSAR) systems are now capable of producing high-quality images of the Earth's surface with meter resolution. The goal of the estimation process is to derive the scene signature from the observed data set. In the case of spatially changing surfaces ("heterogeneous" or "textured" scenes), the first step is to define an appropriate model describing the dependence between the polarimetric signature and the observable as a function of the speckle. In general, the multiplicative model has been employed for POLSAR data processing as a product between the square root of a scalar positive quantity (texture) and the description of an equivalent homogeneous surface (speckle) [1], [2].

Manuscript received January 18, 2011; revised April 27, 2011; accepted May 2, 2011. Date of publication June 9, 2011; date of current version October 28, 2011.

G. Vasile and M. Gay are with the Grenoble Image Speech Signal Automatics Laboratory, Centre National de la Recherche Scientifique, 38402 Grenoble, France (e-mail: gabriel.vasile@gipsa-lab.grenoble-inp.fr; michel.gay@gipsa-lab.grenoble-inp.fr).

F. Pascal is with the SONDRA Laboratory, National University of Singapore/Defence Science and Technology Agency Research Alliance/Supélec, 91192 Gif-sur-Yvette, France (e-mail: frederic.pascal@supelec.fr).

J.-P. Ovarlez and P. Formont are with the Département Électromagnétisme et Radar/Unité Traitement du Signal, Office National d'Études et de Recherches Aerospatiales–The French Aerospace Laboratory, 91761 Palaiseau, France, and also with the SONDRA Laboratory, National University of Singapore/Defence Science and Technology Agency Research Alliance/Supélec, 91192 Gif-sur-Yvette, France (e-mail: ovarlez@onera.fr; pierre.formont@supelec.fr).

Color versions of one or more of the figures in this paper are available online at http://ieeexplore.ieee.org.

Digital Object Identifier 10.1109/LGRS.2011.2152363

In the context of the non-Gaussian polarimetric clutter models, several studies tackled POLSAR parameter estimation using the product model. For deterministic texture, Novak and Burl derived the polarimetric whitening filter (PWF) by optimally combining the elements of the polarimetric covariance matrix to produce a single scalar image [1], [3]. Using the complex Wishart distribution, the PWF for homogeneous surfaces has been generalized to a multilook PWF (MPWF) in [2] and [4]. The objective of this letter is to present a novel parameter estimation technique based on the spherically invariant random vector (SIRV) model. For a detailed review on the use of SIRV with POLSAR data, refer to [5].

This letter is organized as follows. The POLSAR parameter estimation strategy for SIRV clutter model both with normalized texture and normalized covariance matrix is presented in Sections II and III, respectively. Then, the novel span estimator is introduced in Section IV. Next, some estimation results are shown in Section V on a real high-resolution POLSAR data set acquired by the Office National d'Études et de Recherches Aerospatiales (ONERA) Radar Aéroporté Multi-spectral d'Etude des Signatures (RAMSES) system. Eventually, in Section VI, some conclusions are presented.

II. SIRV Clutter Model With Normalized Texture

The SIRV is a class of nonhomogeneous Gaussian processes with random variance [6], [7]. The complex m-dimensional measurement $\mathbf{k}$ (with m being the number of polarimetric channels) is defined as the product between the independent complex circular Gaussian vector $\zeta \sim \mathcal{N}(0, [T])$ (speckle) with zero mean and covariance matrix $[T] = E\{\zeta\zeta^\dagger\}$ and the square root of the positive random variable ξ (representing the texture): $\mathbf{k} = \sqrt{\xi} \cdot \zeta$. It is important to notice that, in the SIRV definition, the probability density function (pdf) of the texture random variable is not explicitly specified. As a consequence, SIRVs describe a whole class of stochastic processes [8].

For POLSAR clutter, the SIRV product model is the product of two separate random processes operating across two different statistical axes [5]. The polarimetric diversity is modeled by the multidimensional Gaussian kernel. The randomness of spatial variations in the radar backscattering from cell to cell is characterized by ξ. Relative to the polarimetric axis, the texture random variable ξ can be viewed as an unknown deterministic parameter from cell to cell.

The texture and the covariance matrix unknown parameters can be estimated from the maximum likelihood (ML) theory. For N independent and identically distributed secondary data,

let $L_{\mathbf{k}}(\mathbf{k}_1,\ldots,\mathbf{k}_N|[T],\xi_1,\ldots,\xi_N)$ be the likelihood function to maximize with respect to $[T]$ and ξ_i

$$L_{\mathbf{k}}(\mathbf{k}_1,\ldots,\mathbf{k}_N;[T],\xi_1,\ldots,\xi_N) = \frac{1}{\pi^{mN}\det\{[T]\}^N} \times \prod_{i=1}^{N}\frac{1}{\xi_i^m}\exp\left(-\frac{\mathbf{k}_i^\dagger[T]^{-1}\mathbf{k}_i}{\xi_i}\right). \quad (1)$$

The corresponding ML estimators are given by [9]

$$\frac{\partial \ln L_{\mathbf{k}}(\mathbf{k}_1,\ldots,\mathbf{k}_N|[T],\xi_1,\ldots,\xi_N)}{\partial\xi_i} = 0 \Leftrightarrow \widehat{\xi_i} = \frac{\mathbf{k}_i^\dagger[T]^{-1}\mathbf{k}_i}{m} \quad (2)$$

$$\frac{\partial \ln L_{\mathbf{k}}(\mathbf{k}_1,\ldots,\mathbf{k}_N|[T],\xi_1,\ldots,\xi_N)}{\partial[T]} = 0 \Leftrightarrow [\widehat{T}] = \frac{1}{N}\sum_{i=1}^{N}\frac{\mathbf{k}_i\mathbf{k}_i^\dagger}{\widehat{\xi_i}}. \quad (3)$$

As the variables ξ_i are unknown, the following normalization constraint on the texture parameters assures that the ML estimator of the speckle covariance matrix is the sample covariance matrix (SCM):

$$[\widehat{T}] = \frac{1}{N}\sum_{i=1}^{N}\mathbf{k}_i\mathbf{k}_i^\dagger = [\widehat{T}]_{SCM} \Leftrightarrow \frac{1}{N}\sum_{I=1}^{N}\mathbf{k}_i\mathbf{k}_i^\dagger\left(1-\frac{1}{\widehat{\xi_i}}\right) = [0_m]. \quad (4)$$

The generalized ML estimator for ξ_i is obtained by introducing (4) in (2)

$$\widehat{\xi_i} = \frac{\mathbf{k}_i^\dagger[\widehat{T}]_{\mathrm{SCM}}^{-1}\mathbf{k}_i}{m}. \quad (5)$$

Note that the $\mathbf{k}_i$ primary data are the cell under study.

The normalized texture estimator from (5) is known as the PWF (PWF-SCM) introduced by Novak and Burl in [1].

III. SIRV Clutter Model With Normalized Covariance Matrix

Now, let the covariance matrix be of the form $[T]=\sigma_0[M]$, such that $\mathrm{Tr}\{[M]\}=1$. The product model can be also written as $\mathbf{k}=\sqrt{\tau}\cdot\mathbf{z}$, where $\mathbf{z}\sim\mathcal{N}(\mathbf{0},[M])$. σ_0 and ξ are two scalar positive random variables such that $\tau=\sigma_0\cdot\xi$.

Using the same procedure as in Section II and given the fact that the covariance matrix is normalized, it is possible to compute the generalized ML estimator of $[M]$ as the solution of the following recursive equation:

$$[\widehat{M}]_{\mathrm{FP}} = f\left([\widehat{M}]_{\mathrm{FP}}\right) = \frac{1}{N}\sum_{i=1}^{N}\frac{\mathbf{k}_i\mathbf{k}_i^\dagger}{\mathbf{k}_i^\dagger[\widehat{M}]_{\mathrm{FP}}^{-1}\mathbf{k}_i}. \quad (6)$$

This approach has been used in [10] by Conte *et al.* to derive a recursive algorithm for estimating the matrix $[M]$. This algorithm consists in computing the fixed point (FP) of f using the sequence $([M]_i)_{i\geq 0}$ defined by

$$[M]_{i+1} = f([M]_i). \quad (7)$$

This study has been completed by the work of Pascal *et al.* [11], [12], which recently established the existence and the uniqueness, up to a scalar factor, of the FP estimator of the normalized covariance matrix, as well as the convergence of the recursive algorithm whatever the initialization. The algorithm can therefore be initialized with the identity matrix $[\widehat{M}]_0=[I_m]$.

The generalized ML estimator (PWF-FP) for the τ_i texture for the primary data $\mathbf{k}_i$ is given by

$$\widehat{\tau_i} = \frac{\mathbf{k}_i^\dagger[\widehat{M}]_{\mathrm{FP}}^{-1}\mathbf{k}_i}{m}. \quad (8)$$

One can observe that the PWF-FP texture from (8) has the same form as the PWF-SCM. The only difference is the use of the normalized covariance estimate given by the FP estimator instead of the conventional SCM [5].

IV. Main Result

The span (total power) σ_0 can be derived using the covariance matrix estimators presented in Sections II and III as

$$\widehat{\sigma_0} = \frac{\mathbf{k}^\dagger[\widehat{M}]_{\mathrm{FP}}^{-1}\mathbf{k}}{\mathbf{k}^\dagger[\widehat{T}]_{\mathrm{SCM}}^{-1}\mathbf{k}}. \quad (9)$$

Note that (9) is valid when considering N identically distributed linearly independent secondary data and one primary data. It can be seen as a double PWF issued from two equivalent SIRV clutter models: with normalized texture variables and with normalized covariance matrix parameter.

The main advantage of the proposed estimation scheme is that it can be directly applied with standard boxcar neighborhoods.

A. Asymptotic Statistics of $\widehat{\sigma_0}$

This section is dedicated to the study of large sample properties and approximations of the span estimator $\widehat{\sigma_0}$ from (9).

On one hand, the asymptotic distribution of the FP estimator from (6) has been derived in [12]. The FP estimator computed with N secondary data converges in distribution to the normalized SCM computed with $N[m/(m+1)]$ secondary data. Since the normalized SCM is the SCM up to a scale factor, we may conclude that, in problems invariant with respect to a scale factor on the covariance matrix, the FP estimate is asymptotically equivalent to the SCM computed with $N[m/(m+1)]$ secondary data. Hence, one can set the degrees of freedom of FP normalized covariance matrix estimators as

$$q_1 = N\frac{m}{m+1}. \quad (10)$$

On the other hand, Chatelain *et al.* established the multisensor bivariate gamma distribution pdf, whose margins are

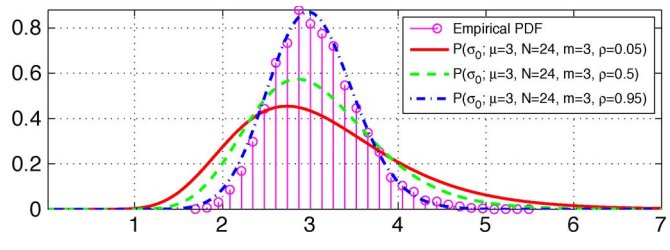

Fig. 1. Ratio pdf of two correlated Gamma random variables (11) for different ρ values and the empirical pdf of simulated σ_0 in Gaussian clutter.

univariate gamma distributions with different shape parameters [13]

$$P_{b\Gamma}(y_1, y_2; p_1, p_2, p_{12}, q_1, q_2).$$

The scale parameters p_2 and p_1 and the shape parameters $q_2 > q_1$ and p_{12} are linked to the mean parameters μ_1 and μ_2, to the number of degrees of freedom n_1 and n_2, and to the normalized correlation coefficient ρ such as

$$q_1 = n_1, q_2 = n_2, p_1 = \frac{\mu_1}{q_1}, p_2 = \frac{\mu_2}{q_2}, p_{12} = \frac{\mu_1\mu_2}{q_1 q_2}(1-\rho).$$

Using these results, we derived the pdf of the ratio $R = y_1/y_2$ of two correlated Gamma random variables

$$\begin{aligned} &P_{R\Gamma}(R, p_1, p_2, p_{12}, q_1, q_2) \\ &\quad = R^{q_1-1}\left(\frac{p_2}{p_{12}}\right)^{q_1}\left(\frac{1}{p_2}\right)^{q_2}\left(\frac{p_{12}}{p_1+Rp_2}\right)^{q_2+q_1}\frac{\Gamma(q_1+q_2)}{\Gamma(q_1)\Gamma(q_2)} \\ &\qquad \times \mathbf{H}_3\left[q_1+q_2, q_2-q_1, q_2;\right. \\ &\qquad\qquad \left. R\frac{p_1p_2-p_{12}}{(p_1+Rp_2)^2}, \frac{p_1p_2-p_{12}}{p_2(p_1+Rp_2)}\right] \end{aligned} \tag{11}$$

where $\mathbf{H}_3(\alpha, \beta, \gamma; x, y) = \sum_{m,n=0}^{\infty}((\alpha)_{2m+n}(\beta)_n/(\gamma)_{m+n} m!n!)x^m y^n$ is one of the 20 convergent confluent hypergeometric series of order two (Horn function) and $(\alpha)_n$ is the Pochhammer symbol such that $(a)_0 = 1$ and $(a)_{k+1} = (a+k)(a)_k$ for any positive integer k [14].

By taking into consideration both (10) and (11) and Cochran's theorem [15], the pdf of the span estimator from (9) converges asymptotically to the the ratio of two correlated Gamma random variable pdfs (the ratio of two quadratics). Moreover, the degrees of freedom n_1 and n_2 are set to $N[m/(m+1)]$ and N (the number of secondary data), respectively.

Fig. 1 shows the behavior of the σ_0 pdf with respect to the normalized correlation coefficient ρ. The pdf parameters are set according to the processing illustrated in Section IV, namely, $N = 24$, $m = 3$, $\mu_1 = 10$, and $\mu_2 = 1$. Notice that, when the normalized correlation coefficient approaches to one, the pdf tends to a Dirac.

A Monte Carlo simulation has also been represented in Fig. 1. Five thousand samples of σ_0 were obtained by computing 5000 $\times$ 24 samples drawn from a zero-mean multivariate circular complex Gaussian distribution with a covariance matrix selected from the real POLSAR data. The span of the selected covariance matrix equals three. One can observe the good correspondence between the empirical pdf of simulated σ_0 and the pdf derived in (11) for $\rho = 0.95$.

TABLE I
EMPIRICAL MEAN AND VARIANCE OF THE σ_0 ESTIMATOR FROM (9) AND THEIR EXPECTED VALUES FOR SIMULATED GAUSSIAN CLUTTER

Boxcar	Expected		Empirical	
	Mean	Variance	Mean	Variance
3×3	3	0	3.42	1.99
5×5			3.13	0.51
7×7			3.04	0.22
9×9			3.03	0.13

Using the same parameters as in the previous Monte Carlo simulation, Table I illustrates the behavior of the empirical mean and variance of the proposed σ_0 in Gaussian clutter (e.g., in homogeneous regions). By using 24 up to 48 secondary data, the estimation bias is negligible, and the empirical variance is close to zero.

B. σ_0 Test

In this section, we propose to show how the estimator from (9) is linked with a binary hypothesis testing problem, also under the following.

1) Null hypothesis H_0: The observed target vector $\mathbf{k} = \sqrt{\xi}\cdot\zeta$ belongs to the SIRV clutter $\zeta \sim \mathcal{N}(0, [T])$ with normalized texture.
2) Alternative hypothesis H_1: The primary target vector $\mathbf{k} = \sqrt{\tau}\cdot\mathbf{z}$ belongs to the SIRV clutter $\mathbf{z} \sim \mathcal{N}(0, [M])$ with normalized covariance matrix.

From the operational point of view, the proposed detector is a classical constant false-alarm-rate detector with current pixel as the primary data and with the local boxcar neighborhood around it as the secondary data.

The Neyman–Pearson optimal detector is given by the following likelihood ratio test (LRT):

$$\Lambda(\mathbf{k}) = \frac{p_{\mathbf{k}}(\mathbf{k}/H_1)}{p_{\mathbf{k}}(\mathbf{k}/H_0)} \underset{H_0}{\overset{H_1}{\gtrless}} \lambda. \tag{12}$$

After expressing the pdf under each hypothesis, it results in

$$\Lambda(\mathbf{k}) = \frac{\frac{1}{\pi^m \det\{[M]\}\tau^m}\exp\left(-\frac{\mathbf{k}^\dagger[M]^{-1}\mathbf{k}}{\tau}\right)}{\frac{1}{\pi^m \det\{[T]\}\xi^m}\exp\left(-\frac{\mathbf{k}^\dagger[T]^{-1}\mathbf{k}}{\xi}\right)} \underset{H_0}{\overset{H_1}{\gtrless}} \lambda. \tag{13}$$

By plugging into the LRT the ML texture estimators from (5) and (8), we obtain

$$\Lambda(\mathbf{k}) = \frac{\det\{[T]\}}{\det\{[M]\}}\left(\frac{\mathbf{k}^\dagger[T]^{-1}\mathbf{k}}{\mathbf{k}^\dagger[M]^{-1}\mathbf{k}}\right)^m \underset{H_0}{\overset{H_1}{\gtrless}} \lambda. \tag{14}$$

Next, we assume that the ratio of determinants is a deterministic quantity, and we denote it by α. This is an approximation, since in practice, the ratio of determinants is also computed using

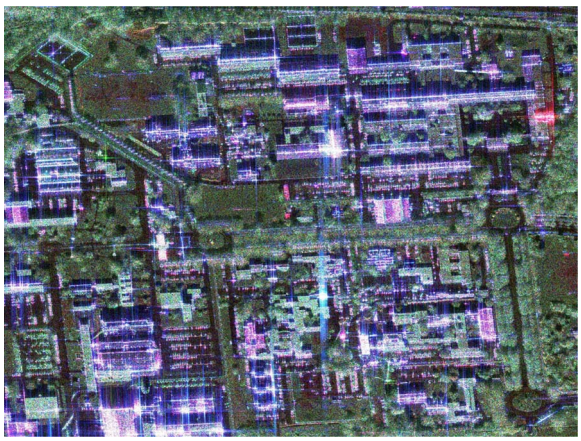

Fig. 2. Toulouse, RAMSES POLSAR data, X-band, 1500 × 2000 pixels: Amplitude color composition of the target vector elements $k_1 - k_3 - k_2$.

the ML estimators of the respective covariance matrix with N secondary data. Finally, by replacing the known covariances by their ML estimates, the generalized LRT is

$$\Lambda(\mathbf{k}) = \alpha \widehat{\sigma_0}^{-m} \underset{H_0}{\overset{H_1}{\gtrless}} \lambda. \tag{15}$$

As α appears as a deterministic quantity only, it is possible to use the pdf derived in Section IV-A to set the decision threshold λ for a specific false-alarm probability.

V. Results and Discussions

The high-resolution POLSAR data set, shown in Fig. 2, was acquired by the ONERA RAMSES system over Toulouse, France, with a mean incidence angle of 50°. It represents a fully polarimetric (monostatic mode) X-band acquisition with a spatial resolution of approximately 50 cm in range and azimuth. In the upper part of the image, one can observe the CNES buildings.

Fig. 4(a)–(c) shows the three SIRV parameters which completely describe the POLSAR data set: the total power, the normalized texture, and the normalized covariance matrix. The 5 × 5 boxcar neighborhood has been selected for illustration; hence, 24 secondary samples and 1 primary data.

Fig. 3 shows the zoom over the red rectangle from Fig. 4(a), where a narrow diplane target was previously detected. Fig. 3(a)–(c) shows the FP-PWF texture, the SCM-PWF normalized texture, and the proposed span estimator $\widehat{\sigma_0}$, respectively. For comparison, the MPWF has been shown in Fig. 3(d). The proposed estimator exhibits better performances in terms of spatial resolution preservation than the MPWF span estimator: The ring effect (two large dips on a spatial profile near the boundaries of a pointwise target [16]) is reduced.

Finally, Fig. 5 shows the detection map obtained using the LRT from (15) with 25 secondary and one primary data. The detection threshold has been obtained by Monte Carlo integration of the pdf from (11) with a false-alarm probability set to $P_{fa} = 10^{-3}$ in each pixel. Note that the pdf integration for such a small P_{fa} is quite time consuming, and fast numerical approximations need to be investigated in the future for going

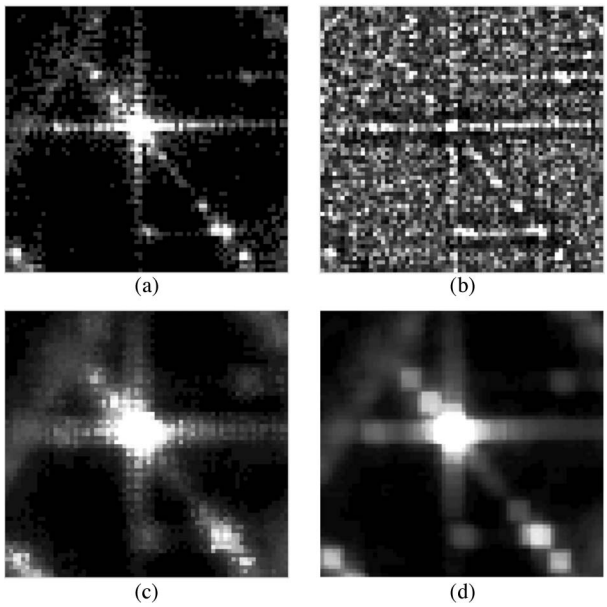

Fig. 3. Toulouse, RAMSES POLSAR data, X-band, 50 × 50 pixels, zoom image: (a) FP-PWF texture, (b) SCM-PWF normalized texture, (c) span estimated using $\widehat{\sigma_0}$ from (9), and (d) SCM-MPWF span.

to an operational level. This detection map can be interpreted as follows:

1) heterogeneous clutter areas, represented in red, reveal dense urban areas, which exhibit fewer dominant scatterers within the resolution cell. Over these areas, according to the hypotheses test from Section IV, it is better to estimate clutter parameters using the normalized covariance SIRV model;
2) homogeneous clutter areas, represented in blue, where the normalized texture model is better.

Concerning the validation of our results, the generalized LRT is known to be asymptotically uniformly most powerful according to the Neyman–Pearson lemma [17]. This "optimality" holds provided that the ML estimators plugged into the LRT are consistent, which is the case for our study [11], [12].

VI. Conclusion

This letter has presented a new estimation scheme for optimally deriving clutter parameters with high-resolution POLSAR images. The heterogeneous clutter in POLSAR data was described by the SIRV model. Three estimators were introduced for describing the high-resolution POLSAR data set: the span, the normalized texture, and the speckle normalized covariance matrix. The asymptotic distribution of the new span estimator has been established. The estimation bias on homogeneous regions has been assessed also by Monte Carlo simulations. Based on these issues, a novel test has been introduced for selecting the most appropriate model for POLSAR heterogeneous clutter described by SIRVs.

This work has many interesting perspectives. We believe that this letter contributes toward the description and the analysis of heterogeneous clutter over scenes exhibiting complex polarimetric signatures. First, the exact texture normalization condition for the PWF-SCM estimator has been derived in Section II under the SIRV clutter hypothesis. A novel

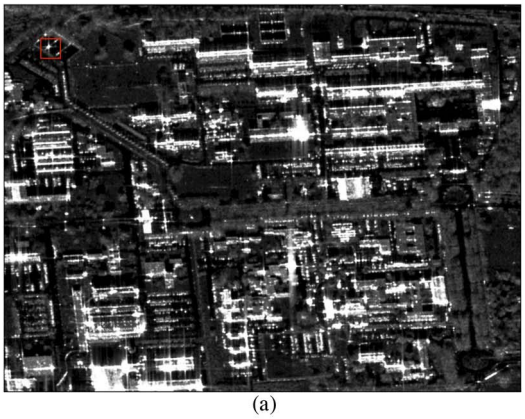

(a)

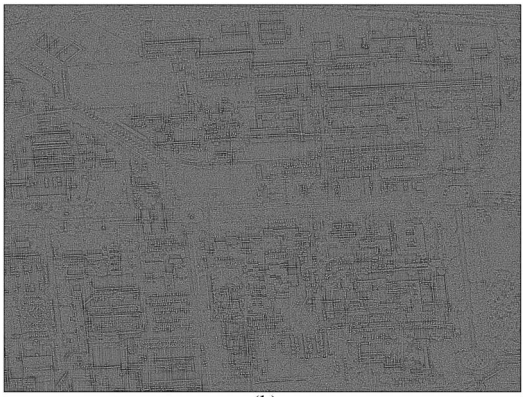

(b)

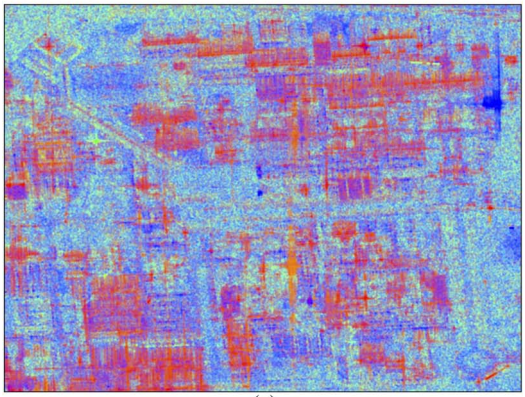

(c)

Fig. 4. Toulouse, RAMSES POLSAR data, X-band, 1500 × 2000 pixels: (a) Span estimated using $\widehat{\sigma_0}$ from (9), (b) normalized texture ξ, and (c) color composition of the normalized coherency diagonal elements $[M]_{11} - [M]_{33} - [M]_{22}$.

estimation/detection strategy has been proposed, which can be used with conventional boxcar neighborhoods directly. Finally, the proposed estimation scheme can be extended to other multidimensional SAR techniques using the covariance matrix descriptor, such as repeat-pass interferometry, polarimetric interferometry, or multifrequency polarimetry.

ACKNOWLEDGMENT

The authors would like to thank Dr. S. Zozor and Dr. F. Chatelain (GIPSA Laboratory, France) for the very fruitful discussions and pieces of advice and Dr. C. Tison (CNES, France) for providing the high-resolution POLSAR images over Toulouse.

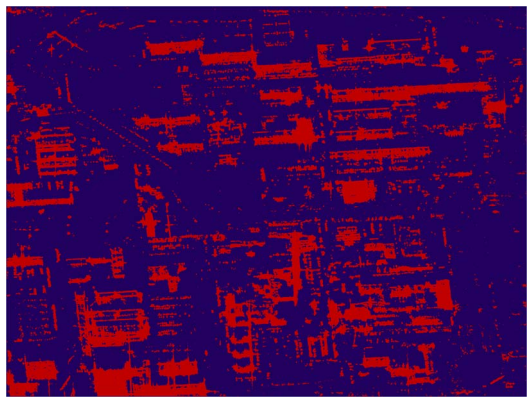

Fig. 5. Toulouse, RAMSES POLSAR data, X-band, 1500 × 2000 pixels: LRT detection map at $P_{fa} = 10^{-3}$ (SIRV with normalized texture in blue and SIRV with normalized covariance in red).

REFERENCES

[1] L. M. Novak and M. C. Burl, "Optimal speckle reduction in polarimetric SAR imagery," *IEEE Trans. Aerosp. Electron. Syst.*, vol. 26, no. 2, pp. 293–305, Mar. 1990.

[2] A. Lopes and F. Sery, "Optimal speckle reduction for the product model in multilook polarimetric SAR imagery and the Wishart distribution," *IEEE Trans. Geosci. Remote Sens.*, vol. 35, no. 3, pp. 632–647, May 1997.

[3] L. M. Novak, M. C. Burl, and W. W. Irving, "Optimal polarimetric processing for enhanced target detection," *IEEE Trans. Aerosp. Electron. Syst.*, vol. 29, no. 1, pp. 234–244, Jan. 1993.

[4] G. Liu, S. Huang, A. Torre, and F. Rubertone, "The multilook polarimetric whitening filter (MPWF) for intensity speckle reduction in polarimetric SAR images," *IEEE Trans. Geosci. Remote Sens.*, vol. 36, no. 3, pp. 1016–1020, May 1998.

[5] G. Vasile, J.-P. Ovarlez, F. Pascal, and C. Tison, "Coherency matrix estimation of heterogeneous clutter in high resolution polarimetric SAR images," *IEEE Trans. Geosci. Remote Sens.*, vol. 48, no. 4, pp. 1809–1826, Apr. 2010.

[6] B. Picinbono, "Spherically invariant and compound Gaussian stochastic processes," *IEEE Trans. Inf. Theory*, vol. IT-16, no. 1, pp. 77–79, Jan. 1970.

[7] K. Yao, "A representation theorem and its applications to spherically-invariant random processes," *IEEE Trans. Inf. Theory*, vol. IT-19, no. 5, pp. 600–608, Sep. 1973.

[8] S. Zozor and C. Vignat, "Some results on the denoising problem in the elliptically distributed context," *IEEE Trans. Signal Process.*, vol. 58, no. 1, pp. 134–150, Jan. 2010.

[9] F. Gini and M. V. Greco, "Covariance matrix estimation for CFAR detection in correlated heavy tailed clutter," *Signal Process.*, vol. 82, no. 12, pp. 1847–1859, Dec. 2002.

[10] E. Conte, A. DeMaio, and G. Ricci, "Recursive estimation of the covariance matrix of a compound-Gaussian process and its application to adaptive CFAR detection," *IEEE Trans. Signal Process.*, vol. 50, no. 8, pp. 1908–1915, Aug. 2002.

[11] F. Pascal, Y. Chitour, J.-P. Ovarlez, P. Forster, and P. Larzabal, "Covariance structure maximum-likelihood estimates in compound Gaussian noise: Existence and algorithm analysis," *IEEE Trans. Signal Process.*, vol. 56, no. 1, pp. 34–48, Jan. 2008.

[12] F. Pascal, P. Forster, J.-P. Ovarlez, and P. Larzabal, "Performance analysis of covariance matrix estimates in impulsive noise," *IEEE Trans. Signal Process.*, vol. 56, no. 6, pp. 2206–2217, Jun. 2008.

[13] F. Chatelain, J. Y. Tourneret, and J. Inglada, "Change detection in multisensor SAR images using bivariate gamma distributions," *IEEE Trans. Image Process.*, vol. 17, no. 3, pp. 249–258, Mar. 2008.

[14] A. Erdlyi, W. Magnus, F. Oberhettinger, and F. Tricomi, *Higher Transcendental Functions*, vol. 1. New York: Krieger, 1981.

[15] W. G. Cochran, "The distribution of quadratic forms in a normal system, with applications to the analysis of covariance," *Math. Proc. Camb. Philos. Soc.*, vol. 30, no. 2, pp. 178–191, 1934.

[16] J. S. Lee, S. R. Cloude, K. P. Papathanassiou, M. R. Grunes, and I. H. Woodhouse, "Speckle filtering and coherence estimation of polarimetric SAR interferometry data for forest applications," *IEEE Trans. Geosci. Remote Sens.*, vol. 41, no. 10, pp. 2254–2263, Oct. 2003.

[17] L. L. Scharf, *Statistical Signal Processing: Detection, Estimation, and Time Series Analysis*. Reading, MA: Addison-Wesley, 1991.